ANODIC ELECTROCHEMICAL PRETREATMENT TIME AND POTENTIAL AFFECT THE ELECTROCHEMICAL CHARACTERISTICS OF MODERATELY BORON-DOPED DIAMOND ELECTRODE

Wei ZHANG[a1,b,*], Shaoai XIE[a2,b], Hongjin CHEN[b1], Mei LI[b2], Li MA[b3] and Jinping JIA[a3,*]

[a] *School of Environmental Science and Engineering, Shanghai JiaoTong University, Dongchuan Rd. 800, Shanghai 200240, China; e-mail: [1] weizhang@sjtu.edu.cn, [2] xie-shaoai@163.com, [3] jinpingjia@126.com*

[b] *School of Chemistry and Chemical Engineering, Shanghai JiaoTong University, Dongchuan Rd. 800, Shanghai 200240, China; e-mail: [1] hjchen@sjtu.edu.cn, [2] meili@sjtu.edu.cn, [3] mali@sjtu.edu.cn*

Received June 11, 2007
Accepted November 27, 2007

Boron-doped diamond (BDD) electrodes, both as-prepared and electrochemically oxidized were studied. The relation between the anodic oxidation treatment time, anodic potential and electrochemical characteristics has been discussed. Electron transfer processes in all BDD electrode surface were studied by cyclic voltammetry. The ferric/ferrous sulfate and ferri/ferrocyanide redox systems were chosen respectively to act as the probe of one-electron transfer processes. The relation between ΔE_p and ψ, the dimensionless parameter, was obtained with a correlation coefficient greater than 0.9987 by mathematics fitting function. The rate constants of the electron transfer reaction, k^0, were evaluated using the ΔE_p values. The k^0 values for all BDD electrodes ranged from 3.33×10^{-5} to 4.72×10^{-5} cm s^{-1} in 0.1 M $FeSO_4$/0.1 M H_2SO_4 and from 1.01×10^{-4} to 2.49×10^{-4} cm s^{-1} in 0.1 M $K_4[Fe(CN)_6]$/0.1 M H_2SO_4 system, which were in the standard range for a quasi-reversible system, respectively. The electrochemical properties of the BDD electrodes changed as a function of the surface anodic treatment time and potential. The anodic oxidation at low potential stripped mainly the impurities of BDD surface, sp^2-carbon, and had little effect on the modification of the surface. While increasing the anodic potential up to +2.0 V, the anodic oxidation stripped the impurities of the BDD surface at first and carried out the modification of the BDD surface from hydrogen-terminated hydrophobic to oxygen-terminated hydrophilic surface with increasing anodic treatment time.

Keywords: Boron-doped diamond electrodes; Anodic electrochemically oxidized treatment time; Anodic potential; Rate constant of electron transfer reaction; Cyclic voltammetry; Electrochemistry; Kinetics.

Electrochemical properties of the boron-doped diamond (BDD) electrode have attracted an ever-increasing number of researchers since it was found

Collect. Czech. Chem. Commun. 2008, Vol. 73, No. 1, pp. 73–87

doi:10.1135/cccc20080073

about 10 years ago[1]. They could possess either semiconducting or semimetallic electronic properties. As a new electrode material, the BDD has shown many unique electrochemical characteristics compared with other carbon materials and metals, including (i) wide working potential window in both aqueous and organic solutions, permitting the investigation of redox processes at extreme potentials, (ii) very low and stable voltammetric background current, enabling high sensitive measurements, (iii) extreme stability of the electrochemical response and relative insensitively to dissolved oxygen, (iv) inert chemical inertness and high resistance to deactivation[2–4].

For such outstanding properties, a number of applications based on BDD electrodes have been reported, especially in electrochemical quantitative analysis. For example, BDD electrodes have been used as a direct amperometric detector to determine many metal ions[5,6] and organic compounds[7–10]. In flow-injection (FI) analysis, liquid chromatography or capillary electrophoresis, BDD electrodes would detect some biopolymers[11,12], drugs[13,14] or pollutants[15]. Furthermore, BDD electrodes have been also used for preparation of glucose sensors[16,17] and wastewater treatments[18,19].

Despite the BDD electrodes possess many superior electrochemical properties, they still have several limitations, such as slow rates of reactions involving adsorption and multi-electron transfer processes[20,21]. In addition, the electrochemical behavior of BDD electrodes strongly depends on the amount and kind of dopants, morphological factors and film defects, the presence of impurities (sp^2-carbon), crystallographic orientation and surface termination (hydrogen or oxygen)[22]. Compared with the influencing factors, the surface termination can be easily controlled by hydrogenation or oxidation of the electrode surface, which usually uses a electrochemical method, plasma treatment or polishing technique[12,23].

The Fijishima research group[23–27] reported that the surface of as-prepared hydrogen-terminated BDD, originally highly hydrophobic, became hydrophilic after the oxygen plasma treatment. It was proved that the electron transfer to redox species on the oxygen-terminated diamond electrodes was changed by cyclic voltammetric curves (CVs) analysis[23]. The carbonyl groups appeared on oxidized BDD surface by anodic polarization or oxygen plasma treatment[24]. The "near-surface" hydrogen was responsible for the quasi-reversible initial response of the ferri/ferrocyanide redox couple, but it became entirely irreversible after oxidation of the BDD surface[25]. The decrease in the electrode activity for both outer-sphere (ferri/ferrocyanide) and inner-sphere (quinone/hydroquinone) redox couples after mild anodic polarization was due to the elimination of "active species" (sp^2-carbon) on

the as-prepared BDD surface[26]. It was proved that passive layers would be generated on the anode oxidized BDD electrodes surface in the impedance studies[27].

The Swain research group[28–30] showed the influence of O-terminations and H-terminations of BDD electrodes on the reversibility of the $[Fe(CN)_6]^{4-/3-}$ and other redox couples. They observed that the electron transfer in the $[Fe(CN)_6]^{4-/3-}$ redox reaction involved a site with the hydrogen-terminated surface, only a quasi-reversible response (ΔE_p = 70 mV) was observed for the H-terminated surface[28]. The $[Fe(CN)_6]^{4-/3-}$ redox couple showed an inner-sphere electron transfer mechanism at BDD electrodes, not the traditional outer-sphere mechanism[29]. The active area of the BDD electrodes increased with the boron doping level[30].

The Avaca research group[22,31] reported that the $K_4Fe(CN)_6/K_3Fe(CN)_6$ system showed reversible transformations after cathodic pretreatment while it behaved in a quasi-reversible manner after anodic polarization[31]. The electrochemical responses of BDD electrodes, after cathodic pretreatment, changed as a function of the time for which they exposed to the atmospheric conditions[22].

In addition, Becker and co-workers[32,33] found that the reversible charge transfer reactions of redox couples occurred at active sites which a partially blocked the BDD electrode surface. Ristein et al.[34] proposed a new surface-transfer doping mechanism consisting in the electron transfers from the valence band of hydrogenated diamond to the adsorbed hydronium ions on the surface, which created the holes for surface conductivity.

To gain a deeper understanding of the relation of electrochemical characteristics and the electrochemical oxidation treatment time and anodic potential in moderately doped polycrystalline diamond electrodes surface, we have undertaken electrochemical measurements of the redox systems, ferri/ferrosulfate and ferri/ferrocyanide redox couples, which acted as the probe of one-electron transfer processes. By CVs analysis, we study the working potential window and the reversibility of the electrode reactions varying with the modification of the BDD surface after different oxidation treatment time and anodic potential. In addition, based on the relation between ΔE_p and ψ, we calculate the rate constants of electron transfer reactions, k^0, and discuss the variation of k^0 values with the different oxidation treatment time and potential.

EXPERIMENTAL

The BDD thin films employed in this work were prepared on silicon (100) wafers substrate using the hot-filament chemical vapor deposition (HF-CVD) technique. The substrate was polished manually with 1 μm diamond particles and then ultrasonically cleaned in acetone and ethanol. Four tantalum wire 0.7 mm in diameter, in series, were used as filaments. The film was grown at approximately 2500 °C (filament temperature) from a gaseous mixture containing 2.0% acetone/H_2 at a pressure of 30 torr. Acetone was used as the carbon source and hydrogen as the carrier gas. B_2O_3, the boron source, was placed uniformly on the rotating tray in the reactor. The thickness of the moderately doped BDD thin film was ca. 2 μm. The film was cooled in hydrogen atmosphere.

Raman spectroscopy was carried out with in backscattering geometry using the polarized 514.5 nm line of an Ar-ion laser with a Raman spectrometer (Jobin Yvon LabRam 800UV, France). Raman scattering measurements have been performed in air at ambient temperature. Surface morphology was observed with a scanning electron microscope (SEM, S-2150, Hitachi, Japan). The water contact angles on the BDD surface were measured using an OCA 20 Contact Angle System (Data Physics Instruments GmbH, Germany) at ambient temperature.

A copper wire was soldered to the edge of BDD electrode using electric gumwater and the epoxy resin was used to fix the electrode surface for obtaining an active electrode area of ca. 0.4 cm^2. Prior to electrochemical studies, the as-prepared BDD electrode was ultrasonically cleaned successively in acetone and ethanol and rinsed with deionized water.

The electrochemical measurements have been performed in a conventional three-electrode cell with a platinum wire used as the counter-electrode and a saturated calomel electrode (SCE) as the reference electrode. Current-potential curves were recorded using the electrochemical workstation (CHI 660C, Shanghai ChenHua Instrument Company, China).

The anodic oxidation treatments were carried out by polarizing the electrode at a potential of +1.0, +1.5, +2.0 and +2.5 V vs SCE in 0.1 M H_2SO_4 solution for 20, 40 and 60 min, respectively.

Solutions were prepared with deionized water, reagents $K_4Fe(CN)_6$, $FeSO_4$ and H_2SO_4 (AR grade) were supplied by Shanghai Chemical Reagent Limit Company.

Experiment temperature: 298 ± 1 K.

RESULTS AND DISCUSSION

Film Characterization

The Raman spectroscopy is highly sensitive in the determination of composition of a diamond film as it can distinguish diamond from different forms of carbon. The Raman spectra for each sample in our work were almost identical (not shown). There is a sharp peak with an average line position being 1329 cm^{-1} over the probed area. A full wave at half maximum (FWHM) is 12–13 cm^{-1} (Fig. 1). Compared with the 1332.5 cm^{-1} peak for a high-temperature, high-pressure reference diamond, the sharp peak shifting to lower wavenumbers is indicative of a slight pull stress[35,36]. The FWHM changing to wider shape are highly sensitive to the doping level and the

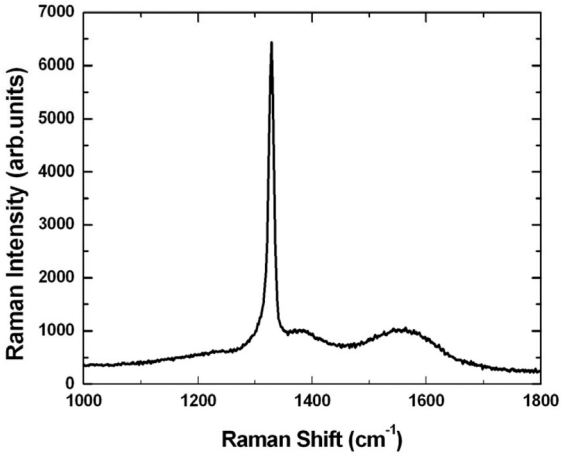

FIG. 1
Raman spectra for the as-prepared (AP) BDD film

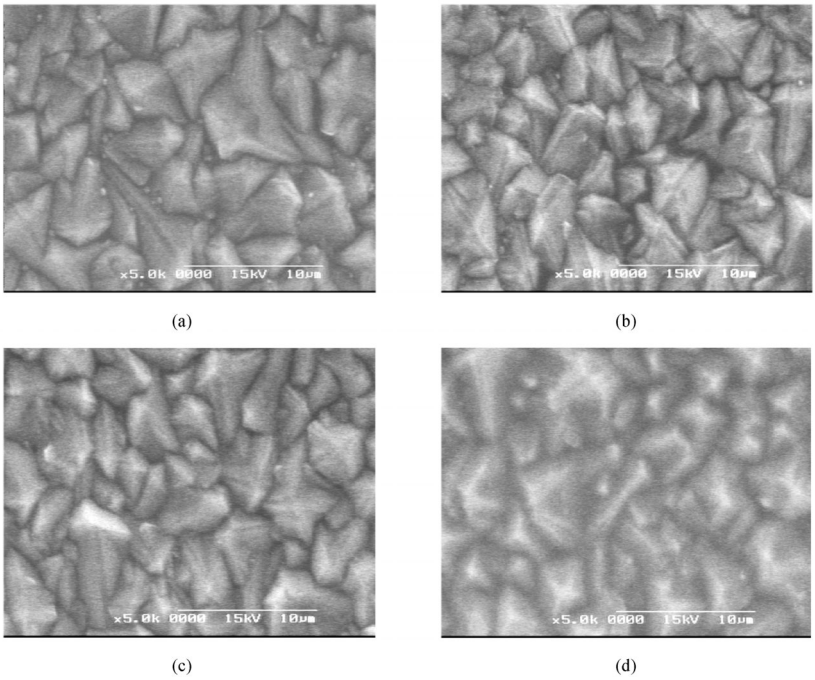

FIG. 2
SEM of BDD electrodes: (a) AP BDD; after EO treatment in a 0.1 M H_2SO_4 solution at +2.5 V for: (b) 20 min (EO-20-2.5V), (c) 40 min (EO-40-2.5V), (d) 60 min (EO-60-2.5V)

disorder content of diamond film[37–39]. The spectra in our work does not show any related band at 1200 cm^{-1}, which is often associated with high boron contents[40]. The diamond lines are very symmetric consistent with a moderate boron-doping level of ca. 10^{19} B cm^{-3}. Moreover, there is also a weak broad peak at 1500–1600 cm^{-1} (see Fig. 1), an indicator of existing sp^2-carbon on the BDD surface[41]. The Raman dispersion effect of sp^2-carbon is 50–80 times higher than that of diamond[42]. Due to the ratio of the peak intensity at 1500–1600 cm^{-1} and 1329 cm^{-1} being ca. 0.154, the level of sp^2-carbon carbon on the BDD surface is low. On the basis of the Raman data analysis, we can suggest that the BDD electrode in our work is a perfect crystalline diamond, moderately boron-doped.

Figure 2 shows SEM photographs of a polycrystalline BDD electrode as-prepared (AP) BDD (Fig. 2a), and after electrochemically oxidation (EO) treatment at 2.5 V and different time (Figs 2b, 2c and 2d).

The image of the AP BDD film exhibited polycrystalline surface, mainly consisting of triangle facets with micron-size crystallites. After EO treatment at 2.5 V for different time, the crystal edges are smoother, and the crystallites shape changes in some sort with increasing EO treatment time.

SEM photographs of EO BDD at the other potentials have almost no change before/after the EO treatment. So, these images are not shown here.

Electrochemical Characteristics

Cyclic voltammetry (CV) analysis is a widely used technique for characterization of BDD electrodes which is able to estimate the working potential window, the reversibility/irreversibility of electrochemical reaction at the BDD surface and some kinetic parameters, like k^0.

The difference in the working potential window of as-prepared (AP) BDD and the electrochemically oxidized (EO) BDD electrodes, anodic treatment times with 20, 40 and 60 min at different anode potentials, respectively, reflects modification of the surface (Fig. 3). Several researchers[26,32,39,43,44] noticed that oxidation treatment significantly decreased the BDD electrode activity because the treatment would remove impurities, such as amorphous sp^2-carbon, which acted as charge transfer mediators of electrolyte breakdown reactions at the BDD electrode. Based on the Raman analysis, there is little sp^2-carbon at BDD electrode surface in our work.

Figure 3 shows that the rates of oxygen evolution, before and after oxidation treatment, are almost the same. This means the oxygen evolution reaction is not sensitive to stripping of small amounts of sp^2-carbon and various surface characters. But hydrogen evolution changes with the oxida-

tion treatment time and potential. After 20 min oxidation treatment, the rates of hydrogen evolution of the EO BDD at different anodic potential are almost the same and the working potential windows are larger than AP BDD (see Fig. 3a). This suggests that the amounts of stripping partly sp^2-carbon at different anodic potential are nearly equal in the first 20 min. When the oxidation treatment time increasing up to 40 min, the hydrogen evolution potential shifts to negative potential with increasing of anodic potential and the potential windows are larger gradually (see Fig. 3b). The measurements of contact angles of water show that the hydrophilicity of EO BDD enhance with increasing anodic potential (data not shown). The H-terminated hydrophobic surface of BDD changes to the O-terminated hydrophilic surface. The sp^2-carbons stripped completely with increasing of anodic potential at that time. Due to the amounts of elimination of sp^2-

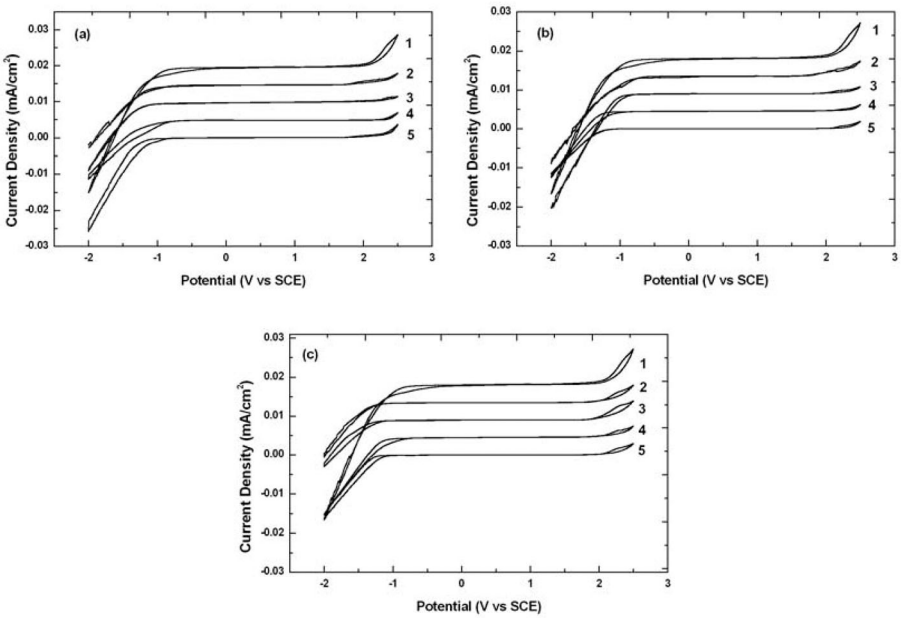

FIG. 3
Cyclic voltammetric curves of AP (curve 1 in Fig. 3a, 3b, 3c) and EO diamond electrodes at different anodic potentials for different treatment times in a 0.1 M H_2SO_4 solution, sweep rate 0.1 V s^{-1}, T = 298 K. EO treatment for: (a) 20 min at +1.0 V (EO-20-1V, curve 2), +1.5 V (EO-20-1.5V, curve 3), +2.0 V (EO-20-2V, curve 4) and +2.5 V (EO-20-2.5V, curve 5); (b) 40 min at +1.0 V (EO-40-1V, curve 2), +1.5 V (EO-40-1.5V, curve 3), +2.0 V (EO-40-2V, curve 4) and +2.5 V (EO-40-2.5V, curve 5); (c) 60 min at +1.0 V (EO-60-1V, curve 2), +1.5 V (EO-60-1.5V curve 3), +2.0 V (EO-60-2V, curve 4) and +2.5 V (EO-60-2.5V, curve 5)

carbon at high anode potential are larger, the effects of hydrophilic surface on the working potential window can be ignored. But at low anodic potential, only a part of sp^2-carbons are stripped and the enhancing of surface hydrophilicity induces the reduction of the working potential window. The working potential window of EO BDD gains a maximum of 3.8 V at high anodic potential of +2.5 V (EO-40-2.5V). Prolonging the oxidation treatment time up to 60 min, at high potential, the H-terminated surface of BDD changes to the O-terminated surface completely, and the working potential windows decrease a little (see Fig. 3c). Compared with anodic potential of +2.0 V, the rate of hydrogen evolution at anode potential of +2.5 V decreases a little. That will be due to the oxidation time at high potential (+2.5 V) is so long that the surface of BDD electrode would be eroded partly to decrease the transfer effect. On the other hand, the working potential

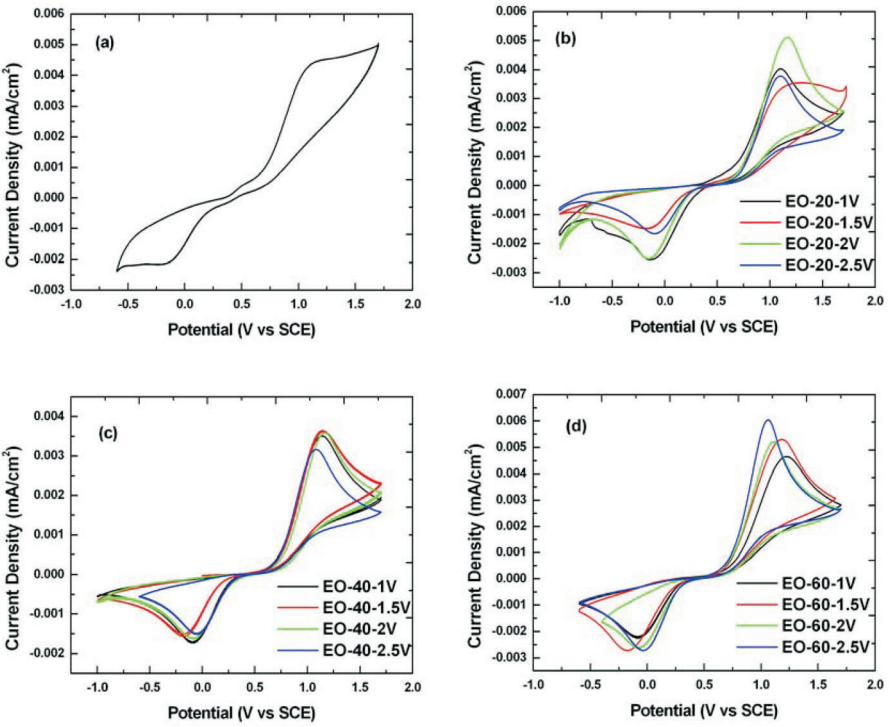

FIG. 4

Cyclic voltammetric curves for AP and EO BDD with different anodic treatment times and potentials in a 0.1 M $FeSO_4$/0.1 M H_2SO_4 solution, sweep rate 0.05 V s^{-1}. (a) AP BDD; after EO treatment at different anodic potentials for: (b) 20 min, (c) 40 min, (d) 60 min

window of EO BDD oxidized at low anodic potential increases significantly. That suggests that the 60 min oxidation treatment time is long enough to strip sp^2-carbons completely at low potential. So, it can be concluded that anodic oxidation at low potential strips mainly the impurities of BDD surface and has little effect on the modification of the surface. While increasing the anodic potential up to +2.0 V, the anodic oxidation strips the impurities of BDD surface at the first time and carries out the modification of the surface with increasing the oxidation time.

Electrochemical activities are examined for diamond electrodes at different anodic oxidation treatment time and potential in a 0.1 M $FeSO_4$/0.1 M H_2SO_4 solution (Fig. 4) and 0.1 M $K_4Fe(CN)_6$/0.1 M H_2SO_4 solution (Fig. 5), respectively.

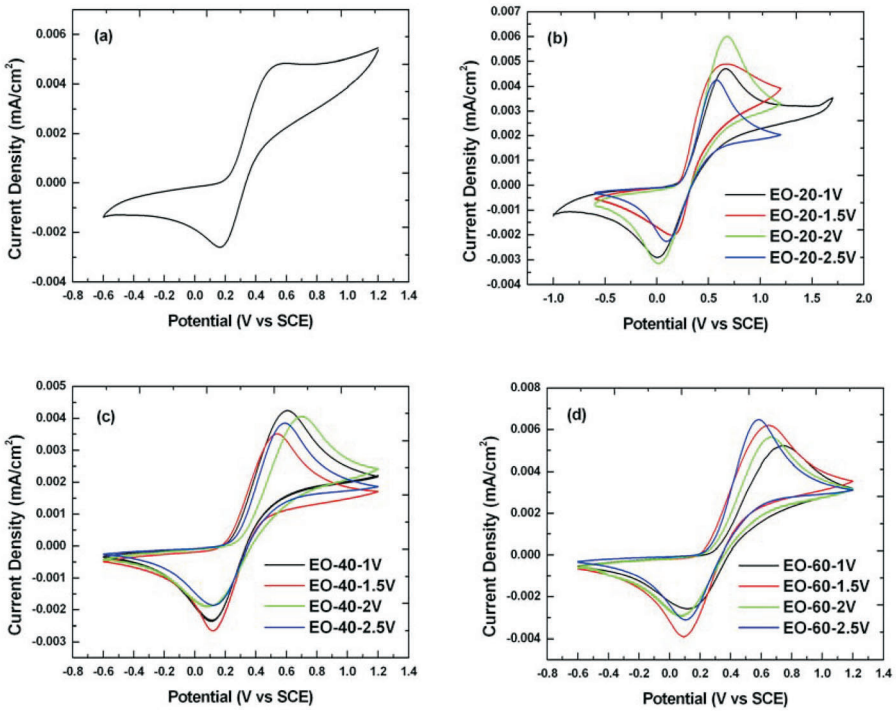

FIG. 5
Cyclic voltammetric curves for AP and EO BDD for different anodic treatment times and potentials in a 0.1 M $K_4Fe(CN)_6$/0.1 M H_2SO_4 solution, sweep rate 0.05 V s^{-1}. (a) AP BDD; after EO treatment at different anodic potentials for: (b) 20 min, (c) 40 min, (d) 60 min

In Fig. 4, it is observed that, compared with the AP BDD electrode, the reversibility of electron transfer reaction of $Fe^{2+/3+}$ redox couples with all EO BDD electrodes is increased. The CV curves exhibit typical quasi-reversibility. The ratio of current peak intensity of anodic reactions, $I_{p,a}$, and that of cathodic reactions, $I_{p,c}$, increases with prolonging EO treatment time at high anodic potential. But the ratio almost does not change at low anodic potentials. That might be that there are more C–O groups produced on the BDD surface at high anodic potential with increasing the oxidation treatment time. So, there might be an attractive ion–dipole interaction between C–O dipoles present at the oxidized diamond surface and positively charged members of the $Fe^{2+/3+}$ couples[24], especially the content of Fe^{2+} is more greater than Fe^{3+} in the solution.

Figure 5 shows that compared with the AP BDD electrode, the reversibility of the electron transfer reaction with all of EO BDD electrodes is increased in $Fe(CN)_6^{3-/4-}$ redox system. The CV curves also exhibit typical quasi-reversibility. The symmetry between anodic and cathodic peaks does not change with increasing EO treatment time at all of the anodic potentials. It is also likely that the repulsive ion–dipole interaction between the C–O dipoles and the negative charged members of the $Fe(CN)_6^{3-/4-}$ (ref.[24]) makes the two type of negative groups bring the same effect on the electron transfer reaction.

In addition, the peak potential, E_p (both anodic and cathodic reaction), would shift to negative or positive potential values with increasing EO treatment time at all of the anodic potentials in the two redox systems. It would be discussed in detail at the next section.

Kinetic Parameters Evaluation

The redox behavior was studied by calculating kinetic parameters of the reaction. For quasi-reversible systems, the evaluation of the rate constant of electron transfer reaction, k^0, as a function of ΔE_p was performed usually by using a data table of variation of $n\Delta E_p$ with the dimensionless parameter, ψ. Parameter ψ is defined by[45]:

$$\psi = \frac{[D_O / D_R]^{\alpha/2} \, k^0}{[D_O \, \pi \nu (nF / RT)]^{1/2}} . \qquad (1)$$

In Eq. (*1*), D_O and D_R are the diffusion coefficients of oxidant and reducer, respectively, α is the transfer coefficient, ν is the sweep rate in CV analysis,

n is the electron number of electron transfer reaction, F is the Faraday constant, R is the gas constant and T is the reaction temperature.

For the $Fe^{2+/3+}$ and $Fe(CN)_6^{4-/3-}$ redox systems, the diffusion coefficients D_O and D_R are considered to be approximately equal. Thus, the ψ values would become independent of the transfer coefficient α. So, basing Eq. (*1*), the k^0 values can be estimated from ψ ones. The approach is closely related to the determination of the electron-transfer kinetics using $n\Delta E_p$ with ν for k^0 in a quasi-reversible system[45]. The ψ values can be evaluated from the data table of typical results of the ψ dependence on $n\Delta E_p$. But the data table involved only a limited part of the $n\Delta E_p$ values, 61–120 mV, in the electrochemical books[45–47]. To obtain more ψ values in a large range of $n\Delta E_p$, we noticed that the dependence of $n\Delta E_p$ on log ψ[46] presented a typical exponential decay behavior. We used the nonlinear fitting function of Origin 6.0 software to obtain the fitting equation for $n\Delta E_p$ and ψ with a correlation coefficient greater than 0.9987:

$$n\Delta E_p = 54.826 + 31.034\, e^{\frac{-\log \psi}{0.6136}} . \qquad (2)$$

This fitting equation permitted the evaluation of ψ values by the $n\Delta E_p$ values. Then the k^0 values could be obtained as a function of the sweep rate from Eq. (*1*) while allowing for literature values of the diffusion coefficient, D_O (7.19×10^{-6} cm^2 s^{-1} for $Fe^{2+/3+}$ and 7.35×10^{-6} cm^2 s^{-1} for $Fe(CN)_6^{4-/3-}$)[48], one electron being involved in the electron transfer process at 298 K. The k^0 values for all BDD electrodes ranged from 3.33×10^{-5} to 4.72×10^{-5} cm s^{-1} in 0.1 M $FeSO_4$/0.1 M H_2SO_4 and from 1.01×10^{-4} to 2.49×10^{-4} cm s^{-1} in 0.1 M $K_4[Fe(CN)_6]$/0.1 M H_2SO_4 system. The results are shown in Fig. 6. Compared with the k^0 standard values for quasi-reversible system[47], $0.3\ \nu^{1/2} \geq k^0 \geq 2 \times 10^{-5}\ \nu^{1/2}$, the k^0 values for all BDD electrodes are in the standard values range.

As shown in Fig. 6a, the k^0 values are changed with the different anodic treatment time and potential in 0.1 M $FeSO_4$/0.1 M H_2SO_4 solution. After the same anodic treatment time, the k^0 values decrease first and then increase with increasing the anodic potential and gain the minimum at 1.5 V. In addition, the k^0 values increase observably with increasing the anodic treatment time at the same anodic potential. This may be due to the stripping of amorphous sp^2-carbon on BDD surface at low anodic potential and producing more C–O groups on the BDD surface at high potential by anodic oxidation. The elimination of sp^2-carbon, which acts as the charge

transfer mediators of electrolyte breakdown reactions at the BDD electrode, decreases the k^0 values. The attractive ion–dipole interaction between C–O dipoles and positively charged members of the $Fe^{2+/3+}$ couples may contribute to acceleration of the $Fe^{2+/3+}$ redox reaction[24].

Figure 6b shows that the k^0 values are changed with the different anodic treatment time and potential in 0.1 M $K_4Fe(CN)_6$/0.1 M H_2SO_4 solution. After anodic treatment, the k^0 values decrease observably. That may be due to the stripping of sp^2-carbon and the repulsive ion–dipole interaction between the C–O dipoles and the negatively charged members of the $Fe(CN)_6^{3-/4-}$ (ref.[24]). Figure 6b also shows that the k^0 values are larger at anodic potential of +1.5 V. This suggests that some C–O groups on the sp^2-carbon would be stripped from the BDD surface with the stripping of sp^2-carbon together at that potential. That would weaken partly the repulsive ion–dipole interaction. In addition, the k^0 values increase little with increasing anodic potential from +2.0 to +2.5 V, which can be considered that the BDD surface after anodic oxidation at high anodic potential would be polished to accelerate the electron transfer reaction.

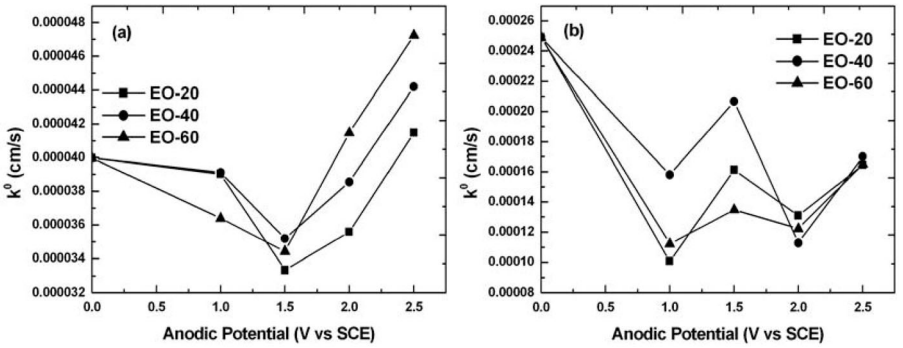

FIG. 6
k^0 as a function of different anodic treatment times and potentials, sweep rate 0.05 V s^{-1} in: (a) 0.1 M $FeSO_4$/0.1 M H_2SO_4 solution, (b) in 0.1 M $K_4Fe(CN)_6$/0.1 M H_2SO_4 solution

CONCLUSION

Electrochemical properties of BDD were found to be strongly influenced by anodic electrochemical treatment of the BDD surface for different anodic treatment time and potential. After the anodic treatment, the BDD surface was transformed from hydrophobic to hydrophilic and electrochemical properties were significantly modified.

By analyzing and calculating the cyclic voltammetric curves for AP and oxidized BDD for different anodic treatment time and potential in 0.1 M $FeSO_4$/0.1 M H_2SO_4 and 0.1 M $K_4Fe(CN)_6$/0.1 M H_2SO_4 solution, respectively, the redox systems exhibit typical quasi-reversibility with all BDD electrodes. The relation between $n\Delta E_p$ and ψ obtained with a correlation coefficient greater than 0.9987. The rate constant of electron transfer reaction, k^0, was evaluated using the $n\Delta E_p$ values. The k^0 values for all BDD electrodes were in the standard range for a quasi-reversible system, which confirmed again that the electrochemical behavior of the chosen redox couples at the AP BDD and anodic oxidation electrodes showed quasi-reversibility. The anodic oxidation at low potential stripped mainly the impurities of BDD surface and had little effect on the modification of the surface. While increasing the anodic potential up to 2.0 V, the anodic oxidation stripped the impurities of BDD surface first and then carried out the modification of the BDD surface from hydrophobic C–H to hydrophilic C–O surface.

This work was supported by the National Nature Science Foundation PR China (Project No. 20477026).

REFERENCES

1. Xu J., Granger M. C., Chen Q., Strojek J. W., Lister T. E., Swain G. M.: *Anal. Chem.* **1997**, *69*, 591A.
2. Strojek J. W., Granger M. C., Dallas T., Holtz M. V., Swain G. M.: *Anal. Chem.* **1996**, *68*, 2031.
3. Lee J., Einaga Y., Fujishima A., Park S.-M.: *J. Electrochem. Soc.* **2004**, *151*, E265.
4. Perret A., Haenni W., Skinner N., Tang X.-M., Gandini D., Comninellis C., Correa B., Foti G.: *Diamond Relat. Mater.* **1999**, *8*, 820.
5. Dragoe D., Spătaru N., Kawasaki R., Manivannan A., Spătaru T., Tryk D. A., Fujishima A.: *Electrochim. Acta* **2006**, *51*, 2437.
6. Manivannan A., Ramakrishnan L., Seehra M. S., Granite E., Butler J. E., Tryk D. A., Fujishima A.: *J. Electroanal. Chem.* **2005**, *577*, 287.
7. Fujishima A., Rao T. N., Popa E., Sarada B. V., Yagi I., Tryk D. A.: *J. Electroanal. Chem.* **1999**, *473*, 179.
8. Martínez-Huitle C. A., Ferro S., De Battisti A.: *Electrochim. Acta* **2004**, *49*, 4027.
9. Pedrosa V. A., Codognoto L., Machado S. A. S., Avaca L. A.: *J. Electroanal. Chem.* **2004**, *573*, 11.
10. Chailapakul O., Popa E., Tai H., Sarada B. V., Tryk D. A., Fujishima A.: *Electrochem. Commun.* **2000**, *2*, 422.
11. Ivandini T. A., Sarada B. V., Terashima C., Rao T. N., Tryk D. A., Ishiguro H., Kubota Y., Fujishimaa A.: *J. Chromatogr., B: Biomed. Appl.* **2003**, *791*, 63.
12. McEvoy J. P., Foord J. S.: *Electrochim. Acta* **2005**, *50*, 2933.

13. Ivandini T. A., Sarada B. V., Terashima C., Rao T. N., Tryk D. A., Ishiguro H., Kubota Y., Fujishima A.: *J. Electroanal. Chem.* **2002**, *521*, 117.
14. Preechaworapun A., Chuanuwatanakul S., Einaga Y., Grudpan K., Motomizu S., Chailapakul O.: *Talanta* **2006**, *68*, 1726.
15. Bouvrette P., Hrapovic S., Male K. B., Luong J. H. T.: *J. Chromatogr., A* **2006**, *1103*, 248.
16. Lee J., Park S.-M.: *Anal. Chim. Acta* **2005**, *545*, 27.
17. Olivia H., Sarada B. V., Honda K., Fujishima A.: *Electrochim. Acta* **2004**, *49*, 2069.
18. Lévy-Clément C., Ndao N. A., Katty A., Bernard M., Deneuville A., Comninellis C., Fujishima A.: *Diamond Relat. Mater.* **2003**, *12*, 606.
19. Panizza M., Micaud P. A., Cerisola G., Comninellis Ch.: *Electrochem. Commun.* **2001**, *3*, 336.
20. Yano T., Popa E., Tryk D. A., Hashimoto K., Fujishima A.: *J. Electrochem. Soc.* **1999**, *146*, 1081.
21. Goeting C. H., Foord J. S., Marken F., Compton R. G.: *Diamond Relat. Mater.* **1999**, *8*, 824.
22. Salazar-Banda G. R., Andrade L. S., Nascente P. A. P., Pizani P. S., Rocha-Filho R. C., Avaca L. A.: *Electrochim. Acta* **2006**, *51*, 4612.
23. Yagi I., Notsu H., Kondo T., Tryk D. A., Fujishima A.: *J. Electroanal. Chem.* **1999**, *473*, 173.
24. Notsu H., Yagi I., Tatsuma T., Tryk D. A., Fujishima A.: *J. Electroanal. Chem.* **2000**, *492*, 31.
25. Tryk D. A., Tsunozaki K., Rao T. N., Fujishima A.: *Diamond Relat. Mater.* **2001**, *10*, 1804.
26. Duo I., Fujishima A., Comninellis Ch.: *Electrochem. Commun.* **2003**, *5*, 695.
27. Kondo T., Honda K., Tryk D. A., Fujishima A.: *Electrochim. Acta* **2003**, *48*, 2739.
28. Granger M. C., Swain G. M.: *J. Electrochem. Soc.* **1999**, *146*, 4551.
29. Granger M. C., Witek M., Xu J., Wang J., Hupert M., Hanks A., Koppang M. D., Butler J. E., Lucazeau G., Mermoux M., Strojek J. W., Swain G. M.: *Anal. Chem.* **2000**, *72*, 3793.
30. Holt K. B., Bard A. J., Show Y., Swain G. M.: *J. Phys. Chem. B* **2004**, *108*, 15117.
31. Suffredini H. B., Pedrosa V. A., Codognoto L., Machado S. A. S., Rocha-Filho R. C., Avaca L. A.: *Electrochim. Acta* **2004**, *49*, 4021.
32. Becker D., Jüttner K.: *J. Appl. Electrochem.* **2003**, *33*, 959.
33. Becker D., Jüttner K.: *Electrochim. Acta* **2003**, *49*, 29.
34. Ristein J., Riedel M., Ley L.: *J. Electrochem. Soc.* **2004**, *151*, E315.
35. Grimsditch M. H., Anastassakis E., Cardona M.: *Phys. Rev. B* **1978**, *18*, 901.
36. Stuart S. A., Prawer S., Weiser P. S.: *Appl. Phys. Lett.* **1993**, *62*, 1227.
37. Peng S. K., Kuang T. C., Cheng X. L., Bai X. J.: *Cemented Carbide* **2001**, *18*, 221.
38. Ager J. W., Walukiewicz W., McCluskey M., Plano M. A., Landstrass M. I.: *Appl. Phys. Lett.* **1995**, *66*, 616.
39. Granger M. C., Xu J., Strojek J. W., Swain G. M.: *Anal. Chim. Acta* **1999**, *397*, 145.
40. Einaga Y., Kim G.-S., Park S.-G., Fujishima A.: *Diamond Relat. Mater.* **2001**, *10*, 306.
41. Sharda T., Vaidaya A., Misre D. S., Bhargava S., Bist H. D., Veluchany P., Minoura H., Selvam P.: *J. Appl. Phys.* **1998**, *83*, 1120.
42. Bhushan B.: *Diamond Relat. Mater.* **1999**, *8*, 1985.
43. Santana M. H. P., De Faria L. A., Boodts J. F. C.: *Electrochim. Acta* **2005**, *50*, 2017.
44. Duo I., Levy-Clement C., Fujishima A., Comninellis C.: *J. Appl. Electrochem.* **2004**, *34*, 935.

45. Bard A. J., Faulkner L. R.: *Electrochemical Methods, Fundamentals and Applications*, p. 243. John Wiley and Sons, New York 2001.
46. Southampton Electrochemistry Group (in Chinese): *Instrumental Methods in Electrochemistry*, p. 191. Fudan University Press, Shanghai 1992.
47. Zhang Z. X., Wang E. K.: *Electrochemical Fundamentals and Methods*, p. 244. Science Press, Beijing 2000.
48. Lide D. R. (Ed.): *Handbook of Chemistry and Physics*, 84th ed., p. 932. CRC Press, New York 2004.